An assessment of optical properties and primary production derived from remote sensing in the Southern Ocean (SO GasEx)

Article *in* Journal of Geophysical Research Atmospheres · July 2011

DOI: 10.1029/2010JC006747

CITATIONS
32

READS
71

11 authors, including:

Zhongping Lee
University of Massachusetts Boston
131 PUBLICATIONS **4,652** CITATIONS
SEE PROFILE

Veronica Lance
National Oceanic and Atmospheric Administration
32 PUBLICATIONS **838** CITATIONS
SEE PROFILE

Shaoling Shang
Xiamen University
52 PUBLICATIONS **1,068** CITATIONS
SEE PROFILE

Robert Vaillancourt
Millersville University
39 PUBLICATIONS **801** CITATIONS
SEE PROFILE

An assessment of optical properties and primary production derived from remote sensing in the Southern Ocean (SO GasEx)

Zhongping Lee,[1] Veronica P. Lance,[2,3] Shaoling Shang,[4] Robert Vaillancourt,[5] Scott Freeman,[6] Bertrand Lubac,[1,7] Bruce R. Hargreaves,[8] Carlos Del Castillo,[9] Richard Miller,[10] Michael Twardowski,[6] and Guomei Wei[4]

Received 22 October 2010; revised 10 March 2011; accepted 20 April 2011; published 22 July 2011.

[1] Optical properties and primary production were measured during the Southern Ocean (SO) Gas Exchange Experiment (GasEx) (March–April 2008). To assess and evaluate these properties derived from remote sensing, absorption coefficients derived from remote sensing reflectance (R_{rs}) with the quasi-analytical algorithm were compared with those from in situ measurements from both an ac-9 optical instrument deployed on a profiling package and from discrete water samples analyzed using filter pad spectrophotometry. Total absorption coefficients from R_{rs} retrievals were found, on average, to be ~12% less than ac-9 measurements and ~15% less than filter pad measurements. Absorption coefficients of gelbstoff-detritus and phytoplankton pigments (at 443 nm) derived from R_{rs} were ~15% and ~25% less than ac-9 measurements, respectively. The difference can be well explained based on the determination methods and these results indicate general consistency between remote sensing retrievals and in situ measurements for these waters. Further, incorporating measured surface radiation data, water column primary production (PP_{eu}) was estimated using chlorophyll concentration based models (Chl-PP) and a phytoplankton absorption based model (Aph-PP), where remote-sensing Chl was retrieved with an operational empirical algorithm. These estimated PP_{eu} values were then compared with primary productivity measured using ^{14}C incubation techniques, and coefficient of determination (R^2, N = 13) of 0.74 were found for the Aph-PP results, while the R^2 of the Chl-PP results were less than 0.5. Such a contrast further highlights the importance of analytically retrieving phytoplankton absorption from measurement of ocean color and the advantage of using phytoplankton absorption to represent the role of phytoplankton in photosynthesis. Spatial distribution and contrast of PP_{eu} in the greater SO GasEx region estimated from satellite data are also presented.

Citation: Lee, Z., et al. (2011), An assessment of optical properties and primary production derived from remote sensing in the Southern Ocean (SO GasEx), *J. Geophys. Res.*, *116*, C00F03, doi:10.1029/2010JC006747.

1. Introduction

[2] Phytoplankton photosynthesis in the ocean (primary production) modulates the impact of anthropogenic carbon on the climate and environment. *Sabine et al.* [2004] have shown that the oceans can take up about half of the anthropogenic carbon dioxide from the atmosphere. Detailed information about the temporal and spatial variation of primary production is thus essential for studying and understanding air-sea CO_2 exchange that are influenced by the "biological pump" [*Arrigo et al.*, 2008; *Behrenfeld et al.*, 2002; *Falkowski et al.*, 2003; *Platt and Sathyendranath*, 1988]. This spatial and temporal variability, however, cannot be adequately addressed over regional and global scales using traditional water sample methods due to extreme undersampling in time and space. Satellite sensors, though not ideal in characterizing the ocean water column, are the

[1]Geosystems Research Institute, Mississippi State University, Stennis Space Center, Mississippi, USA.
[2]Lamont-Doherty Earth Observatory, Columbia University, Palisades, New York, USA.
[3]Now at Science Systems and Applications, Inc., NASA Goddard Space Flight Center, Greenbelt, Maryland, USA.
[4]State Key Laboratory of Marine Environmental Science, Xiamen University, Xiamen, China.
[5]Department of Earth Sciences, Millersville University of Pennsylvania, Millersville, Pennsylvania, USA.
[6]Department of Research, WET Labs, Inc., Narragansett, Rhode Island, USA.
[7]Now at Environnements et Paléoenvironnements Océaniques et Continentaux, UMR 5805, University of Bordeaux1, Talence, France.
[8]Department of Earth and Environmental Sciences, Lehigh University, Bethlehem, Pennsylvania, USA.
[9]Ocean Remote Sensing Group, Applied Physics Laboratory, Johns Hopkins University, Laurel, Maryland, USA.
[10]Department of Geological Sciences and Institute for Coastal Science and Policy, East Carolina University, Greenville, North Carolina, USA.

0148-0227/11/2010JC006747

only option available for global scales, now and into the foreseeable future [*Platt and Sathyendranath*, 1988]. For this reason, the estimation of primary production from satellite measurements of ocean color radiometry is critical for developing an understanding of how ocean biological processes affect, and are affected by, changes in atmospheric radiative budgets and global biogeochemical cycles [*Falkowski*, 1998; *Platt and Sathyendranath*, 1988]. Because of these critical needs and their importance in biological oceanography and carbon cycle studies, large efforts have been made worldwide to study oceanic primary production (PP), with unprecedented and more realistic results obtained regarding primary production of the global oceans [*Antoine et al.*, 1995, 1996; *Arrigo et al.*, 1998; *Behrenfeld et al.*, 1998; *Behrenfeld et al.*, 2006; *Ishizaka*, 1998; *Longhurst et al.*, 1995; *Morel and Berthon*, 1989; *Platt and Sathyendranath*, 1988; *Sathyendranath et al.*, 1991, 1995].

[3] Although a wide variety of models for the calculation of ocean productivity from ocean color have been developed [*Balch et al.*, 1989; *Behrenfeld and Falkowski*, 1997a; *Campbell et al.*, 2002; *Carr et al.*, 2006; *Cullen*, 1990], no consensus has emerged among the practitioners as to which approach(es) should be used in global applications. *Behrenfeld and Falkowski*'s [1997b] model has become *a de facto* standard, although it has been found deficient in various environments [e.g., *Marra et al.*, 2003; *McClain et al.*, 2002; *Ondrusek et al.*, 2001]. In short, accurate assessment of productivity from space is still a daunting challenge [*Balch and Byrne*, 1994]. This is also true for the Southern Ocean [*Arrigo et al.*, 1998, 2008; *Moore and Abbott*, 2000].

[4] Waters in the Southern Ocean, due to an abundance of major nutrients, contribute significantly to the global primary production [*Arrigo et al.*, 2008; *Takahashi et al.*, 2002]. Under the Joint Global Ocean Flux Study (JGOFS), many investigations were made of the physical and biogeochemical parameters that affect the air-sea CO_2 fluxes in the Southern Ocean [*Treguer and Pondaven*, 2002]. These studies concluded that the Southern Ocean acts as a significant net sink for atmospheric CO_2 [*Arrigo et al.*, 1998, 2008; *Takahashi et al.*, 1999; *Treguer and Pondaven*, 2002]. For example, the region south of 50°S contributes ~20% of the global CO_2 sink [*Takahashi et al.*, 2002], which clearly demonstrates the significance of Southern Ocean on the global biogeochemical carbon cycle.

[5] However, these earlier studies also pointed out "substantial uncertainty about the processes and factors that regulate primary productivity, and particularly its variability, in the Southern Ocean" [*Treguer and Pondaven*, 2002]. When compared to a two-layer biogeochemical model [*Schlitzer*, 2002], chlorophyll based models underestimate primary productivity by a factor of ~2–5 in the Southern Ocean [*Arrigo et al.*, 1998; *Longhurst et al.*, 1995] (similar observations were also found for other regions [*Ducklow*, 2003]). Recent estimates using satellite data were also found much lower than earlier evaluations [*Arrigo et al.*, 2008]. Errors from both biogeochemical model [*Schlitzer*, 2002] and satellite PP estimation contribute to this quite large discrepancy. In particular, numerous studies [*Clementson et al.*, 2001; *Dierssen and Smith*, 2000; *Garcia et al.*, 2005; *Mitchell and Holm-Hansen*, 1990; *Mitchell et al.*, 1991; *Sullivan et al.*, 1993] have shown that there are large discrepancies between ratio-derived chlorophyll-a concentration (Chl) and in situ Chl in the Southern Ocean, although this discrepancy may be reduced if in situ Chl is measured using high-performance liquid chromatography (HPLC) rather than the more common fluorescence/acidification method [*Marrari et al.*, 2006]. Nevertheless, any Chl error will impact the estimation of primary production because Chl is one of the most important variables in nearly all primary production models [*Behrenfeld and Falkowski*, 1997a, 1997b; *Campbell et al.*, 2002; *Carr et al.*, 2006; *Platt and Sathyendranath*, 1988].

[6] To bypass the uncertainties associated with the empirically estimated Chl, a different strategy to estimate PP using phytoplankton absorption (a_{ph}) has been set forth [*Lee et al.*, 1996; *Marra et al.*, 2007], a strategy that requires robust retrieval of optical properties from the measurement of ocean color. A test [*Lee et al.*, 1996] with data collected during the Marine Light–Mixed Layer (MLML) program, although quite limited in measurements, showed promising results when PP based on semianalytically derived a_{ph} was compared with the PP based on ratio-derived Chl. These MLML results thus inspired a possibility of significantly reducing the uncertainty of remotely estimated PP by focusing on and improving the optical properties derived from remote sensing [*International Ocean-Colour Coordinating Group* (*IOCCG*), 2006] and developing PP model parameters centered on phytoplankton absorption coefficient [*Marra et al.*, 2007].

[7] Following this path and general strategy, we took the opportunity provided by the Southern Ocean (SO) Gas Exchange Experiment (GasEx) (28 February to 8 April 2008) (D. Ho et al., Southern Ocean Gas Exchange Experiment: Setting the stage, submitted to Journal of Geophysical Research, 2011) to evaluate the retrieval of optical properties, and more importantly, to test and evaluate the competence of these two approaches in estimating PP from remote sensing. This analysis is significant also because this region is extremely undersampled for the necessary bio-optical properties, and accurate optical properties are key to determining the light field for photosynthesis. Here we present results of both optical properties and primary production derived from spectral remote sensing and their comparison with those from in situ measurements.

2. Data and Methods

[8] During the SO GasEx (D. Ho et al., submitted manuscript, 2011), measurements of remote sensing reflectance and primary production, along with numbers of measurements of other optical properties were made at about 10 stations (see Figure 1 for sample locations). The following describes measurement methods for each property, while Table 1 summarizes the matchups of the location/time and general information.

2.1. Optical Properties From In Situ Measurements

2.1.1. Absorption From ac-9

[9] Optical profiles to 120 m were conducted on 15 days with a package that included several scattering instruments (ECO-BB3, ECO-VSF, MASCOT, WET Labs, Inc.) and an ac-9 (WET Labs, Inc.) to measure beam attenuation, absorption, and scattering at 9 wavelengths. Two profiles were made at each site, one with whole water and one with a

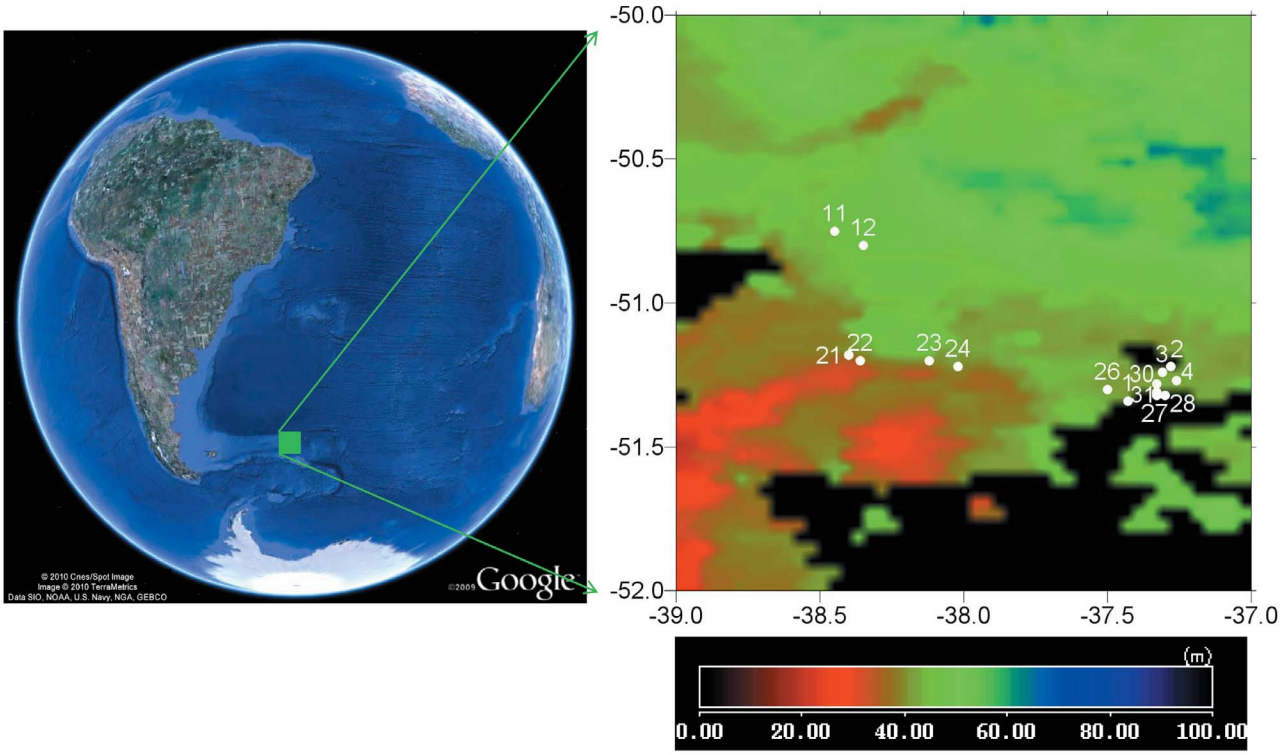

Figure 1. Locations and dates of the optical/bio-optical measurements during SO GasEx. Color image is the euphotic zone depth of March 2008 (derived from MODIS Aqua, monthly composite, provided by Ocean Biology Processing Group).

0.2 μm filter in series to remove particles. Particulate absorption (a_p, m^{-1}) was calculated by subtracting filtered absorption coefficient (which is the absorption coefficient of gelbstoff measured in the field: a_g, m^{-1}) from whole absorption coefficient (the sum of particle and gelbstoff absorption coefficient, a_{pg}). Since the absorption coefficient of pure water (a_w, m^{-1}) was removed during calibration, we added a_w to a_{pg} for each wavelength to calculate total absorption coefficient (a, m^{-1}). Wavelengths used for this analysis are 412, 443, and 488 nm, which are sensitive to changes of in-water constituents, and they were considered identical to the wavelengths used for remote sensing retrievals (410, 440, 490 nm) for simple description. Correction for particle scattering in the unfiltered profiles was done using the proportional method of *Zaneveld et al.* [1994], and the standard temperature and salinity corrections were made [*Sullivan et al.*, 2006]. For this analysis, the top 15 m were judged to be the surface sample, and values were averaged within this range.

[10] For the ac-9 data, absorption coefficient of phytoplankton pigments (a_{ph}, m^{-1}) was derived from the measured particle absorption coefficient (a_p) by assuming an a_{ph} to a_p ratio as 0.92, 0.94, and 0.96 for 412, 443, and 488 nm, respectively. These values were the average of the a_{ph}/a_p obtained from filter pad measurements described below. And the difference between a_p and a_{ph} (resulting in a_d, m^{-1}) were added to the ac-9 measured a_g to form a_{dg}.

2.1.2. Absorption From Filter Pad Method

[11] Discrete seawater samples were collected twice daily with the CTD-rosette package (<2 h apart from ac-9 measurements) and processed immediately. Samples were filtered on GF/F for immediate analysis of spectral absorption using the transmittance (T)-reflectance (R) filter pad method [*Tassan and Ferrari*, 1995; *Tassan et al.*, 1997]. The instrument used for measuring %T and %R was a custom fiber optic spectrophotometer consisting of 50 mm Reflectance Integrating Sphere (Avantes, Inc), UV-VIS diode array spectrometer (Ocean Optics USB-2000, 3.7 μm bandwidth FWHM), and UV-VIS xenon flash lamp (Ocean Optics PX-2) using OOIBase32 software, Spectralon® 99% reflectance standard, and holmium oxide solution in a sealed cuvette for wavelength calibration. Correction for filter pad scattering (beta correction) was established postcruise [*Hargreaves and Vaidya*, 2010; *Vaidya*, 2010] using a center mount integrating sphere to measure spectral absorbance of algal cultures (whole and GF/F filtrate) for comparison with filter pad OD based on transmittance and reflectance. Total particulate absorption coefficient (a_p) was measured within several hours after sample collection and then filters were bleached (1% sodium hypochlorite in isotonic sodium sulfate artificial seawater). Phytoplankton pigment absorption coefficient (a_{ph}) was estimated by subtracting bleached spectral absorption (a_d) from unbleached spectral absorption.

2.1.3. Absorption of Gelbstoff

[12] Discrete samples were also filtered through 47 mm 0.2 μm nylon filters (Whatman Nuclepore) and CDOM absorption (a_g) measured using an Ultrapath (WPI, Inc) system. The Ultrapath consists of a single beam optical path that contains a high-intensity deuterium and halogen light

Table 1. Date, Location, and Matchup of Measurements

Month	Day	Latitude (S)	Longitude (W)	In Situ R_{rs}	ac-9	Filtered ac-9	Sample a_{ph} and a_d	Sample a_g	Surface Chl (mg m^{-3})	PP[a] (mg C m^{-2} d^{-1})	MODIS
Mar	11	−50.75	−38.45	X			X		0.91	566.1	
Mar	12	−50.80	−38.35	X	X	X	X	X	0.91	492.8	
Mar	21	−51.22	−38.4	X	X	X					
Mar	22	−51.22	−38.36	X	X		X	X	1.04	473.0	
Mar	23	−51.22	−38.12	X	X	X	X	X	0.72	236.3	
Mar	24	−51.22	−38.02						0.62	397.7	X
Mar	26	−51.3	−37.5	X	X		X	X	0.43	164.8	
Mar	27	−51.32	−37.33	X	X		X	X	0.48	223.8	
Mar	28	−51.32	−37.3	X					0.40	202.3	
Mar	30	−51.28	−37.33	X	X	X			0.47	224.9	
Mar	31	−51.31	−37.33	X			X	X	0.51	235.2	
Apr	1	−51.34	−37.43	X	X	X	X	X	0.53	310.1	
Apr	2	−51.37	−37.48	X			X	X	0.49	299.1	
Apr	3	−51.41	−37.52	X	X	X	X	X		337.2	X
Apr	4	−51.45	−37.44	X	X	X	X	X	0.51	362.0	

[a]Reproduced from Lance et al. (unpublished manuscript, 2011).

source, a multiple path length (2, 10, 50, 200 cm) liquid waveguide, and a fiber optic spectrometer (Tidas-1, WPI Inc). Optical density spectra (250–721 nm) were acquired using the 2 m path length cell following *Miller et al.* [2002]. Reference optical density spectra were made using Milli-Q water. Sample spectra were corrected for refractive index effects caused by salinity and temperature variations [*Miller et al.*, 2002]. Corrected absorption spectra a_g were added to a_d described above to yield estimates of a_{dg} for discrete water samples.

2.2. Shipboard Remote-Sensing Reflectance

[13] Remote-sensing reflectance ($R_{rs}(\lambda)$, defined as ratio of water-leaving radiance to downwelling irradiance just above the surface, sr^{-1}) was calculated from measurements made above the sea surface as described by *Carder and Steward* [1985]. Specifically, upwelling radiance (L_u) and downwelling sky radiance (L_{sky}) were measured with a handheld spectroradiometer, and viewing the water and sky at 30° from vertical and 90° from the solar plane, respectively. Downwelling irradiance was derived by measuring the radiance (L_R) reflected from a standard diffuse reflector (Spectralon®). For each water and sky scan, total remote-sensing reflectance ($T_{rs}(\lambda)$, sr^{-1}) and sky reflectance ($S_{rs}(\lambda)$, sr^{-1}) were derived with

$$T_{rs} = \frac{L_u}{L_R}\frac{R_R}{\pi} \quad \text{and} \quad S_{rs} = \frac{L_{sky}}{L_R}\frac{R_R}{\pi}, \tag{1}$$

with R_R the reflectance of the diffuse reflector (Spectralon, ~10%).

[14] Based on these measured T_{rs} and S_{rs} curves, averages of T_{rs} and S_{rs} for each station were obtained after rejecting obvious outliers. T_{rs} represents the sum of water-leaving radiance and surface-reflected sky radiance. $R_{rs}(\lambda)$ is then calculated as [*Austin*, 1974; *Carder and Steward*, 1985; *Lee et al.*, 2010a]

$$R_{rs}(\lambda) = T_{rs}(\lambda) - F\,S_{rs}(\lambda) - \Delta, \tag{2}$$

where F is surface Fresnel reflectance (around 0.023 for the viewing geometry), and Δ accounts for the residual surface contribution (glint, etc.). For SO GasEx (clear oceanic waters), Δ was determined by assuming R_{rs} around 750 nm as 0.

2.3. On-Deck Primary Production

[15] During the SO GasEx cruise primary productivity was measured by two different methods using ^{14}C tracer: by 24 h incubations of ^{14}C-spiked seawater in incubators exposed to ambient irradiance on the aft deck of the research vessel ("on-deck method"), and by short-duration photosynthesis-irradiance experiments ("P-E method"). A complete description of the on-deck method is given by V. P. Lance et al. (Primary productivity, new productivity and carbon export during two Southern Ocean Gas Exchange (SO GasEx) Lagrangian tracer experiments, unpublished manuscript, 2011), and for the P-E method of R. C. Hamme et al. (Dissolved O2/Ar and other methods reveal rapid changes in productivity during a Lagrangian experiment in the Southern Ocean, submitted to *Journal of Geophysical Research*, 2011). Brief descriptions are given here. As measurement from the 24 h incubation represents daily production better [*Halsey et al.*, 2010], the data from the 24 h incubation is used to evaluate remote sensing models (section 4.2).

[16] Primary productivity (on-deck method) was estimated from discrete water samples collected on predawn casts using standard ^{14}C uptake measurements in 24 h, on-deck incubations with six simulated light depths (70, 39, 33, 22, 9, 3.3, and 1%) then discrete values were integrated to the 1% euphotic light depth (see Lance et al. (unpublished manuscript, 2011) for details). Incident PAR irradiance (μEin m^{-2} s^{-1}) was measured at 5 s intervals and averaged for 15 min records using a pair of LI-192uw cosine response quantum sensors and a LI-1000 data logger from LI-COR, Inc. Incident PAR irradiance was integrated over the exposure period for each experiment for use in calculating PAR-specific photosynthesis rates.

[17] Short-term (1–2 h) incubation (P-E method) was also carried out during the cruise, where midmorning CTD casts

(~10:00 LT) were used to collect seawater for the P-E experiments. Seawater samples were spiked with 10 μCi of ^{14}C bicarbonate and incubated in a radial photosynthetron for 1–2 h under blue-filtered artificial light. As the focus of this study is daily primary production, results from these short-term experiments were not included in this article.

2.4. Satellite Data

[18] To get a regional understanding, PP_{eu} of 1 March to 31 May 2008 (austral autumn) in the greater SO GasEx region were estimated from satellite measurements using inputs (Chl, Sea Surface Temperature (SST), and Photosynthetic Available Radiation (PAR)) acquired from NASA (http://oceancolor.gsfc.nasa.gov). All of the three inputs are recently reprocessed data products of Moderate Resolution Imaging Spectroradiometer (MODIS) (Version r2009.1), with Chl retrieved using the OC3M algorithm [*O'Reilly et al.*, 2000], and SST from the radiance measurement at 4 μm (SST). Remote sensing reflectance from MODIS were also acquired from NASA and fed to the quasi-analytical algorithm (QAA) scheme (see section 3.1) to derive IOPs. The spatial resolution of these data was 4.5 × 4.5 km, and 8 day composite data were used. All these input fields were interpolated to a 1/6° × 1/6° grid before they were fed to the PP models (see section 3.2).

[19] PP_{eu} of 2 days (24 March and 3 April), when both MODIS and in situ PP_{eu} measurements were available, was also estimated from remote sensing measurements (see section 3.2). Daily MODIS R_{rs}, Chl, SST and PAR data with 1.1 × 1.1 km spatial resolution were downloaded from the same web site and fed to the QAA and PP models.

3. Derivation of Properties From Remote Sensing

3.1. Inherent Optical Properties

[20] For the derivation of inherent optical properties (IOPs, absorption and backscattering coefficients in particular), the quasi-analytical algorithm (QAA) developed by *Lee et al.* [2002] was applied. Specifically, to better separate the contributions of molecular and particle scatterings to R_{rs}, a modified analytical function for R_{rs} was implemented

$$R_{\mathrm{rs}}(\lambda,\Omega) = \left(G_0^w(\Omega) + G_1^w(\Omega)\frac{b_{\mathrm{bw}}(\lambda)}{\kappa(\lambda)}\right)\frac{b_{\mathrm{bw}}(\lambda)}{\kappa(\lambda)} + \left(G_0^p(\Omega) + G_1^p(\Omega)\frac{b_{\mathrm{bp}}(\lambda)}{\kappa(\lambda)}\right)\frac{b_{\mathrm{bp}}(\lambda)}{\kappa(\lambda)}, \quad (3)$$

with $\kappa = a + b_b$, and $b_b = b_{bw} + b_{bp}$. Here Ω represents the Sun-sensor angular geometry for the remote-sensing reflectance. The total absorption and backscattering coefficients are a and b_b, respectively, while b_{bw} is the backscattering coefficient of pure seawater (all m^{-1}). Values of the model parameters (G_0^w (Ω), G_1^w (Ω), G_0^p (Ω), and G_1^p (Ω); sr^{-1}) for various Sun angles and viewing geometries have been developed based on Hydrolight simulations [*Lee et al.*, 2011].

[21] In the inversion process, the backscattering and absorption coefficients of pure seawater are based on *Morel* [1974] and *Pope and Fry* [1997], respectively. When the total absorption coefficient was decomposed into the contributions of phytoplankton and detritus-gelbstoff [*Lee et al.*, 2002], the ratio of $a_{ph}(412)/a_{ph}(443)$ and the ratio of $a_{dg}(412)/a_{dg}(443)$ were estimated following QAA-v5 (see http://www.ioccg.org/groups/Software_OCA/QAA_v5.pdf).

3.2. Primary Production

[22] The absorption-based production model (designated as Aph-PP in the following) was described by *Lee et al.* [1996]. For illustration purpose, and to simplify the calculations, a spectrally integrated formulation for PP at depth z is used here

$$PP(z) = \varphi_m \frac{K_\varphi \exp(-v \times E(z))}{K_\varphi + E(z)}[\mathrm{Aph} \times E(z)], \quad (4)$$

with

$$E(z) = E_0 \exp(-K_{\mathrm{PAR}}(z) \times z). \quad (5)$$

The term associated with φ_m and K_φ on the right side of equation (4) represents the vertical variation of the quantum yield of photosynthesis. Values of the model parameters used were $\varphi_m = 0.12$ mg C · Ein^{-1}, $K_\varphi = 10$ Ein m^{-2} d^{-1}, and $v = 0.01$ (Ein m^{-2} d^{-1})$^{-1}$. Aph on the right side of equation (4) is the absorption coefficient of phytoplankton at 443 nm, which represents the blue peak of spectral a_{ph}. $E(z)$ in equations (4) and (5) is the PAR value at depth z, with E_0 for surface PAR. $K_{\mathrm{PAR}}(z)$ is the vertical attenuation coefficient of PAR, which is modeled as a function of absorption and backscattering coefficients [*Lee et al.*, 2005]. Water column PP (PP_{eu}) was then calculated by integrating $PP(z)$ between 0 and 50 m. This nominal 50 m water column is slightly deeper than the euphotic zone depths (~35–41 m) for the stations considered here. Primary production estimated from this approach is represented as Aph-PP.

[23] Numerous models [*Arrigo et al.*, 2008; *Behrenfeld and Falkowski*, 1997a; *Campbell et al.*, 2002; *Carr et al.*, 2006; *Friedrichs et al.*, 2009; *Platt and Sathyendranath*, 1988] have been developed to estimate PP based on the concentration of chlorophyll (Chl-PP in the following text). To demonstrate and compare PP results estimated from remote sensing using both Aph-PP and Chl-PP approaches, PP_{eu} from two Chl-PP based models were also produced. One is the widely used VGPM [*Behrenfeld and Falkowski*, 1997b]

$$\mathrm{PP_{eu}} = 0.66125 \times P^B_{\mathrm{opt}} \times \frac{E_0}{E_0 + 4.1} \times Z_{\mathrm{eu}} \times Chl \times DL. \quad (6)$$

[24] Z_{eu} in equation (6) is euphotic zone depth (in m) and was estimated using QAA-derived absorption and backscattering coefficients [*Lee et al.*, 2007]. Day length (DL) was taken as 11.5 h. For estimation of PP_{eu} from in situ R_{rs}, $P^B_{\mathrm{opt}} = 2.8$ mg C (mg Chl)$^{-1}$ h^{-1} was used (higher than the actual ~1.5 mg C mg Chl^{-1} h^{-1} in situ estimates of P^B_{opt} during SO GasEx). This value was estimated from *Behrenfeld and Falkowski* [1997b] with a water temperature of 5°C, as the temperature was in a range of 4.7–5.3°C during the experiment. When evaluating spatial variation of PP_{eu} from satellite data, values of P^B_{opt} were estimated based on MODIS SST information as described by *Behrenfeld and Falkowski* [1997b]. Primary production estimated from this approach is represented as Chl-PP_B.

Table 2a. Statistical Results Between R_{rs}-Derived and ac-9-Measured Properties

Property	Wavelength (nm)	N	Range	δ (%)	R^2
Total absorption coefficient (a) (m^{-1})	412	10	0.093–0.163	11.2	0.64
	443	10	0.085–0.135	12.5	0.73
	488	10	0.062–0.093	13.2	0.80
Phytoplankton absorption coefficient (a_{ph}) (m^{-1})	412	7	0.018–0.058	35.5	0.55
	443	7	0.027–0.062	24.5	0.74
	488	7	0.026–0.052	46.9	0.83
Detritus-gelbstoff absorption coefficient (a_{dg}) (m^{-1})	412	7	0.058–0.100	14.0	0.78
	443	7	0.045–0.072	15.1	0.76
	488	7	0.017–0.029	19.4	0.75

[25] The other model is the one developed by *Arrigo et al.* [2008] that targeted specifically waters in the Southern Ocean

$$\mathrm{PP_{eu}} = \mathrm{Fun}(\mathrm{Chl}, E_0, \mathrm{SST}). \tag{7}$$

[26] The *Arrigo et al.* [2008] model is time, depth, and wavelength resolved. To facilitate the calculation with ocean color remote sensing and daily integrated irradiance data (E_0), the model is modified to a time-, depth-, and wavelength-integrated form (see Appendix A for details). Primary production estimated from this approach is represented as Chl-$\mathrm{PP_A}$.

[27] In the calculations of PP by equations (4), (6), and (7), Aph, Z_{eu} and Chl were derived from R_{rs}, which was either measured in situ or acquired from MODIS, so did values of E_0.

4. Results and Discussion

[28] We use two statistical measures to assess and quantify comparisons between remote sensing products with in situ measurements. The first is the coefficient of determination (R^2) evaluated in linear scale and the second is percentage difference (δ) derived from the root mean square deviation (RMSD) and calculated as follows:

$$\mathrm{RMSD} = \sqrt{\mathrm{AVERAGE}\left[\log_{10}\left(\frac{Q_{\mathrm{insitu}}}{Q_{\mathrm{inversion}}}\right)\right]^2}, \tag{8}$$

$$\delta = \left(10^{\mathrm{RMSD}} - 1\right) \times 100\%. \tag{9}$$

Here Q represents a property evaluated, and the log transform places an equal evaluation between overestimated and underestimated results. Values of R^2 and δ for each property are summarized in Tables 2 and 3.

4.1. Optical Properties

4.1.1. General Description

[29] Because optical properties determine the propagation of light from sea surface to deeper depths for photosynthesis, consistent results of IOPs between in situ and remote sensing are essential to the goal of understanding the spatial and temporal variations from satellite measurements. As there are two sets of in situ IOPs (one from ac-9 and one from water samples, and note that the values from the two determinations are not identical), remote sensing retrievals are compared with both measurements. Statistical results are summarized in Tables 2a and 2b and comparisons are shown in Figures 3–5. Generally, the statistical results indicate that it is more consistent (higher R^2 and lower δ values) between remote-sensing retrievals and ac-9 measurements (Table 2a) whereas there are larger differences between remote-sensing retrievals and water sample measurements (Table 2b). This could be because both R_{rs} and ac-9 measure the total optical signal in the upper water column, while measurements from water samples (which provide a direct measurement of each component) divide the total signal into separate components first (via physical and/or chemical separations) and then sum the individuals for total signal. Because each and every step of the measurements will introduce uncertainties, larger uncertainties would be expected for a product with more steps associated with its derivation/determination.

[30] For waters included in this study (Table 1), the variabilities of $a(443)$, $a_{ph}(443)$, and $a_{dg}(443)$ from ac-9 measurements are rather small (Table 2a). The ~0.085 to 0.135 m^{-1} range (from ac-9 measurements) of $a(443)$ indicates that these waters are significantly less clear compared to waters in the South Pacific gyre where $a(443)$ is around 0.015 m^{-1} [*Bricaud et al.*, 2010; *Morel et al.*, 2007]. This assertion is further supported by the range of Z_{eu} (~35 to 41 m) of the waters studied. However, the ~1.6 high:low ratio of the total absorption coefficient at 443 nm (after removing pure water value) became ~2.3 high:low ratio for $a_{ph}(443)$. This difference is because the ratio of $a_{dg}(443)$/$a_{ph}(443)$ is not a constant, but spanned a range of ~0.6 to 1.6 (~1.0 to 2.0 from ac-9 measurements, see Figure 2) even for this relatively small open ocean area. This observation echoes a generally noncovarying nature between a_{dg} and a_{ph} in the oceans [*Hu et al.*, 2006; *Morel and Gentili*, 2009], which in turn will impact the retrieval of Chl via empirical spectral ratios and then PP estimation in the oceans (see more discussions in section 4.2).

4.1.2. Absorption Coefficient of the Total

[31] Total absorption coefficient is the most important component that determines the color of a water body and the attenuation from surface to depth. For the total absorption

Table 2b. Statistical Results Between R_{rs}-Derived and Properties Measured From Water Samples

Property	Wavelength (nm)	N	Range	δ (%)	R^2
Total absorption coefficient (a) (m^{-1})	412	10	0.106–0.148	11.2	0.50
	443	10	0.094–0.122	11.9	0.53
	488	10	0.067–0.085	16.9	0.57
Phytoplankton absorption coefficient (a_{ph}) (m^{-1})	412	11	0.032–0.049	34.6	0.52
	443	11	0.035–0.059	46.9	0.52
	488	11	0.026–0.044	57.8	0.56
Detritus-gelbstoff absorption coefficient (a_{dg}) (m^{-1})	412	10	0.052–0.101	24.7	0.48
	443	10	0.036–0.070	22.2	0.44
	488	10	0.018–0.035	21.3	0.44

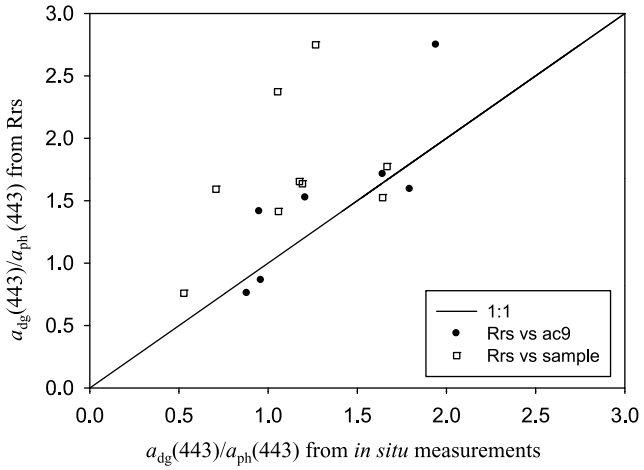

Figure 2. Variation of $a_{dg}(443)/a_{ph}(443)$ measured during SO GasEx. Also shown is a comparison between $a_{dg}(443)/a_{ph}(443)$ from in situ measurement and $a_{dg}(443)/a_{ph}(443)$ derived from remote sensing.

coefficients of the waters in this study, the δ values are ~15% when R_{rs} retrievals are compared with those from both ac-9 and sample measurements, which indicate generally consistent results between in situ measurements and remote sensing derivations (also see Figure 3 and Tables 2a and 2b). This is particularly significant because error is expected for each of the three methods of determination [*Lee et al.*, 2010b; *Leymarie et al.*, 2010; *Tassan and Ferrari*, 1995]. Better agreement is found for $a(412)$, while R_{rs}-derived $a(443)$ and $a(488)$ are generally lower than those from in situ measurements. The reason(s) for this spectral bias is(are) not yet clear.

4.1.3. Absorption Coefficient of Phytoplankton and Detritus-Gelbstoff

[32] The δ of a_{ph} is higher than that of the total absorption and that of detritus-gelbstoff absorption coefficients when R_{rs} retrieval is compared with values derived from ac-9 data (Table 2a) or compared with values from sample measurements (Table 2b). This discrepancy is due in part to errors or uncertainties in each method. For example, additional uncertainties are associated with the filtering of water samples and subsequent determination of a_{ph} (see section 2.1) and a_{dg}. Also, when total absorption is decomposed into the contribution of individual components in R_{rs} retrieval, the associated spectral shape parameters are not known and must be determined empirically [*IOCCG*, 2006], thus introducing errors/uncertainties to the remotely derived a_{ph} [*Lee et al.*, 2010b]. Furthermore, because $a_{dg}(443)$ generally contributed more to $a(443)$ than $a_{ph}(443)$ did for these waters, a small error in $a_{dg}(443)$ could result in bigger error in $a_{ph}(443)$. More detailed analyses and discussions about the QAA inversion, and remote sensing of IOPs in general, are given by *Lee et al.* [2010b] and *IOCCG* [2006]. Nevertheless, a δ value about 20% with an R^2 value ~0.75 for both $a_{ph}(443)$ and $a_{dg}(443)$ (comparison between R_{rs} retrieval and ac-9 measurements) suggest consistent and satisfactory determinations for these properties, at least for measurements during this experiment.

[33] Larger discrepancies were found for both $a_{ph}(488)$ and $a_{dg}(488)$ between R_{rs} retrievals and measurements (Figures 4 and 5). The δ values are 46.9% and 19.4% for $a_{ph}(488)$ and $a_{dg}(488)$ (see Table 2a), respectively, between R_{rs} retrieval and ac-9 data; and they are 57.8% and 21.3% for $a_{ph}(488)$ and $a_{dg}(488)$ (see Table 2b), respectively, between R_{rs} retrieval and water sample data, and the R^2 values are higher between R_{rs} retrievals and ac-9 measurements than that between R_{rs} retrieval and water sample

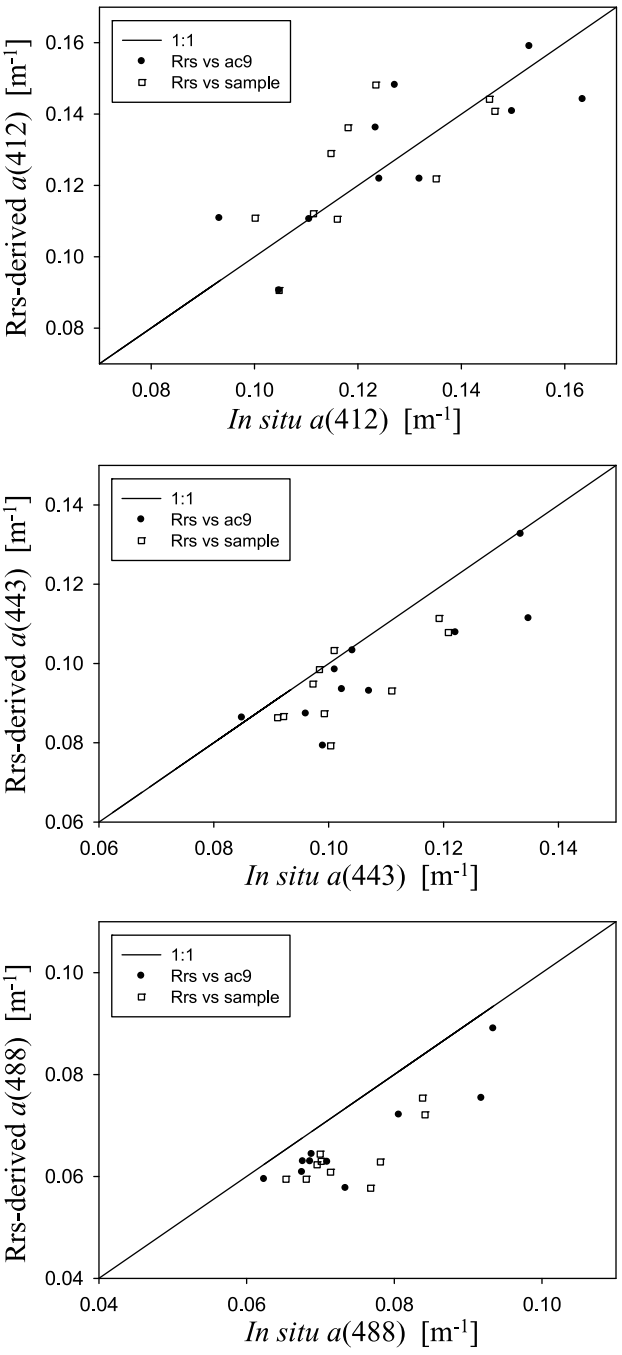

Figure 3. Comparison of total absorption coefficients between measured in situ (ac-9 and water samples) and derived (QAA) from R_{rs}.

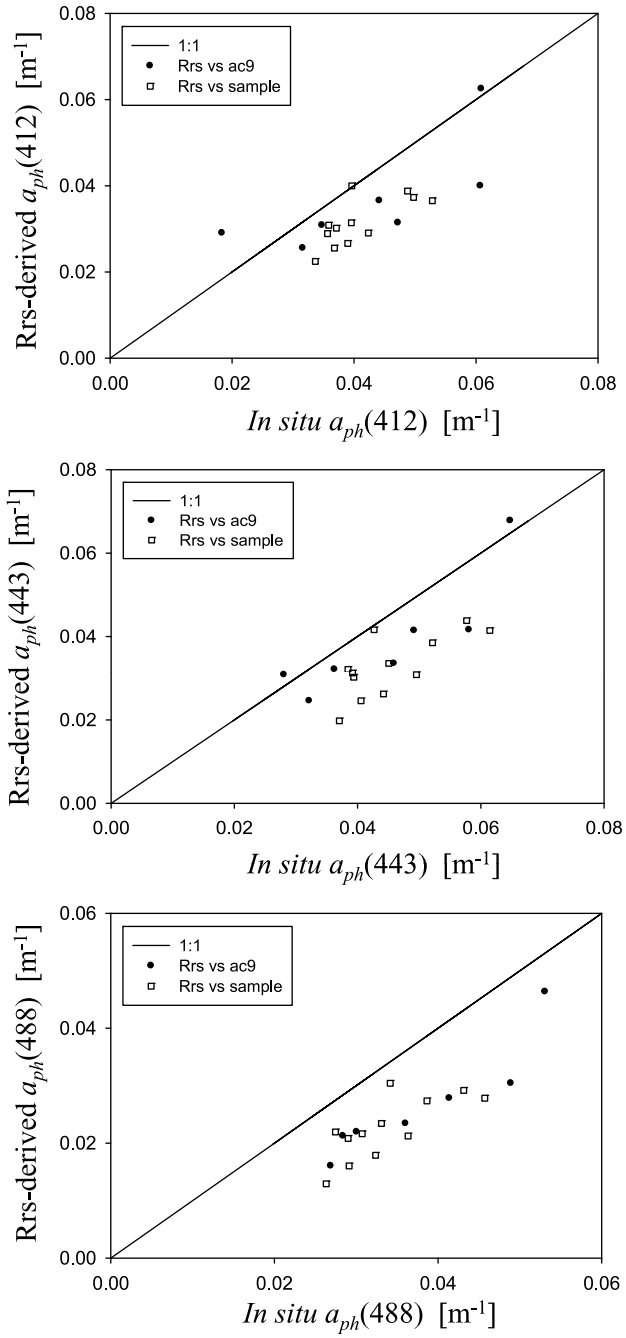

Figure 4. Same as Figure 3 but for phytoplankton absorption coefficients.

results. The a_{dg}(488) from R_{rs} is slightly higher while a_{ph}(488) is much lower than those from ac-9 measurements. In the QAA inversion system, a_{dg}(488) is estimated from the QAA-derived a_{dg}(443) with a spectral slope (~0.016 nm^{-1} for these stations, not shown) estimated empirically from R_{rs} (QAA-v5). The spectral slope of a_g is found to be ~0.019 nm^{-1} between 443 and 488 nm from ac-9 measurements (~0.014 nm^{-1} between 412 and 443 nm), and a_d contributed less than 5% to a_{dg} based on measurements of water samples. Thus the slope of a_{dg} used in QAA is slightly less than that from measurements for the 443–488 nm range, which explains, in part, the slightly higher a_{dg}(488) from R_{rs} by QAA. On the other hand, a_{ph}(488) is the result of QAA-derived a(488) minus a_w(488) and the above derived a_{dg}(488). The lower a(488) compounded with the higher a_{dg}(488) from R_{rs} results in an even lower a_{ph}(488) (Figure 4, bottom). These results highlight, assuming limited/no error of in situ measurements, the importance of obtaining accurate information of the spectral shapes of the individual components in analytical

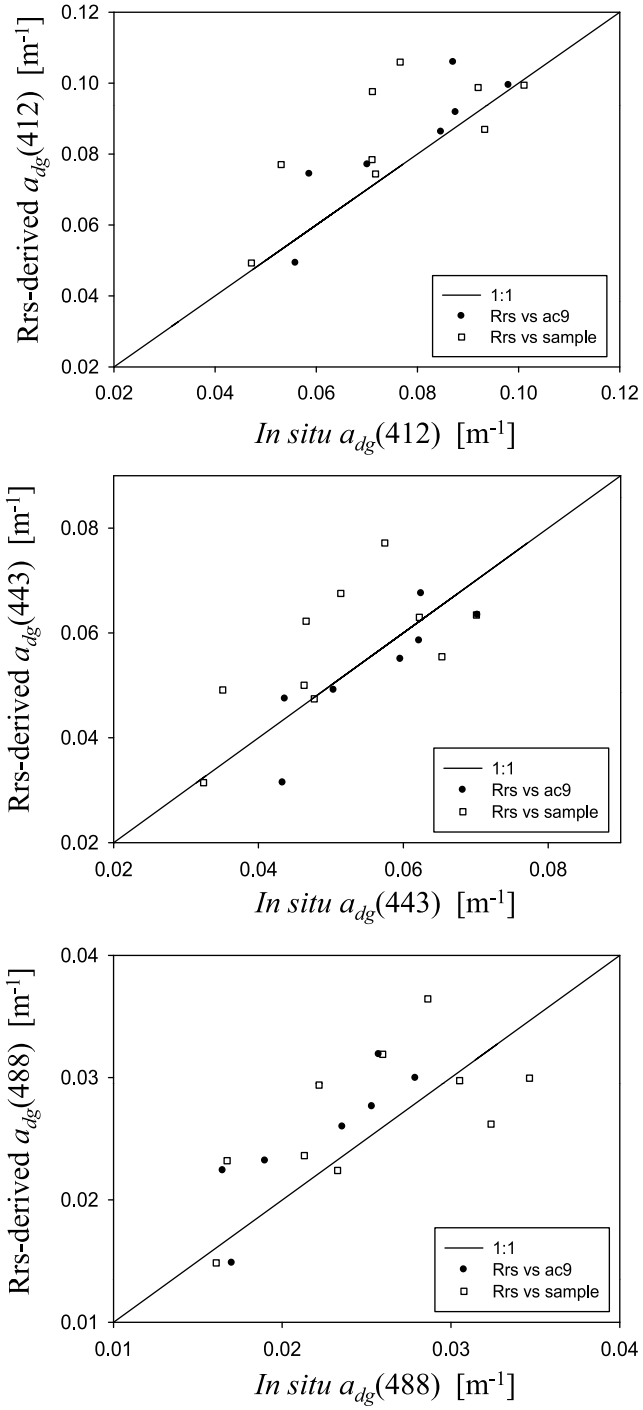

Figure 5. Same as Figure 3 but for detritus-gelbstoff absorption coefficients.

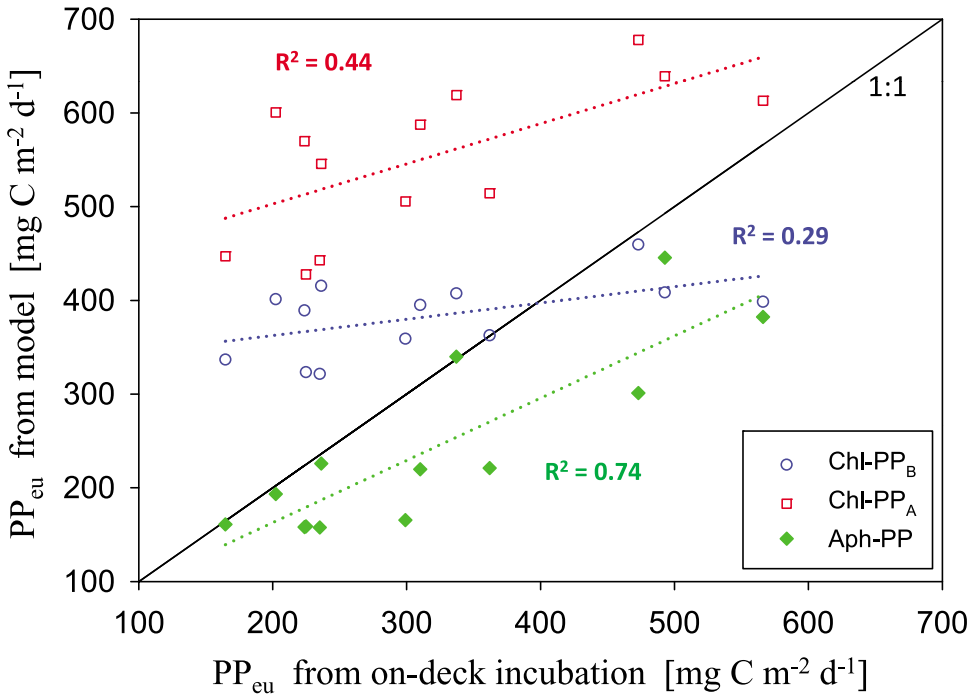

Figure 6. Comparison between PP_{eu} measured and PP_{eu} derived from remote sensing. Green symbols are results from Aph-PP, blue symbols are results from Chl-PP_B, and red symbols are results from Chl-PP_A. Dotted lines show linear regression results of the three pairs and R^2 values are presented in their corresponding colors.

ocean color inversion in order to achieve accurate derivation of spectral IOPs from R_{rs}.

4.2. Primary Production

4.2.1. Comparison With In Situ Measurements

[34] The PP_{eu} values estimated by both Chl-PP and Aph-PP approaches were compared with those from primary productivity measurements made by traditional shipboard ^{14}C techniques (see Figure 6), and the coefficient of determination (R^2) of each approach is presented in Table 3. As a crude evaluation of the quantity of estimated PP_{eu}, δ values regarding PP_{eu} from the three models (which were 0.29 for Aph_PP, 0.35 for Chl-PP_B, and 0.49 for Chl-PP_A) were also included in Table 3. However, because value of δ directly depends on the values used for either P^B_{opt} or G_{max} (for Chl-PP) or φ_m (for Aph-PP), and the default values included in the Chl-PP and Aph-PP models are not necessarily optimized for the waters in this study (for instance, value of P^B_{opt} used was higher than the value measured in situ), value of δ may not yet measure the robustness of models presented here.

[35] The value of R^2, however, has no dependence on P^B_{opt} or G_{max} or φ_m and provides a measure of the power of each model in explaining the variability of PP_{eu}. For measurements made during SO GasEx, it is found that the PP_{eu} variation was explained much better with the Aph-PP model (R^2 = 0.74, N = 13) than with the two Chl-PP models (R^2 = 0.29 and 0.44, N = 13, respectively) when both Aph and Chl were derived from R_{rs} with widely used algorithms. This is not surprising, because, when implementing the Chl-PP model, Chl was derived from a simple spectral ratio (OC3M) of measured R_{rs} (and presently this is the operational algorithm for MODIS), a practice that cannot separate the impacts of detritus-gelbstoff absorption to R_{rs} and cannot cope with the spatial/temporal variations of chlorophyll-specific absorption coefficient [*Bricaud et al.*, 1995; *Sathyendranath et al.*, 1987; *Stuart et al.*, 1998]. Figure 7a compares Chl from R_{rs} ratio with Chl from water samples (measured via HPLC technique), and shows that Chl values from R_{rs} are nearly constant for the waters where Chl varied in a range of ~0.4–1.0 mg m^{-3}. Statistically, the R^2 value is 0.23 (N = 12) and δ is 33.4% between the ratio-derived and measured Chl of this data set. These evaluations indicate that the R_{rs} ratio did not capture the variation of Chl for those waters, and rather largely affected by relatively high gelbstoff-detritus contributions (see Figure 2). If we compare the R_{rs} ratio-derived Chl with QAA-derived a(488) (for these waters, the actual ratio used for empirical Chl derivation is $R_{rs}(488)/R_{rs}(550)$ as $R_{rs}(488) > R_{rs}(440)$), the R^2 value is 0.88 (N = 12). Because the uncertainty of analytically derived a(488) is limited for oceanic waters [*Lee et al.*, 2010b], the high R^2 value between ratio-derived Chl and QAA-derived a(488) further stresses that a value calculated from empirical R_{rs} ratio predominantly represents the total

Table 3. Statistical Results Between PP_{eu} Estimated From Remote Sensing and PP_{eu} Measured From On-Deck Incubation

	N	Range	Approach	δ	R^2
Depth-integrated primary production (mg C m^{-2} d^{-1})	13	~165–566	Chl-PP_B	0.35	0.29
	13	~165–566	Chl-PP_A	0.49	0.44
	13	~165–566	Aph-PP	0.29	0.74

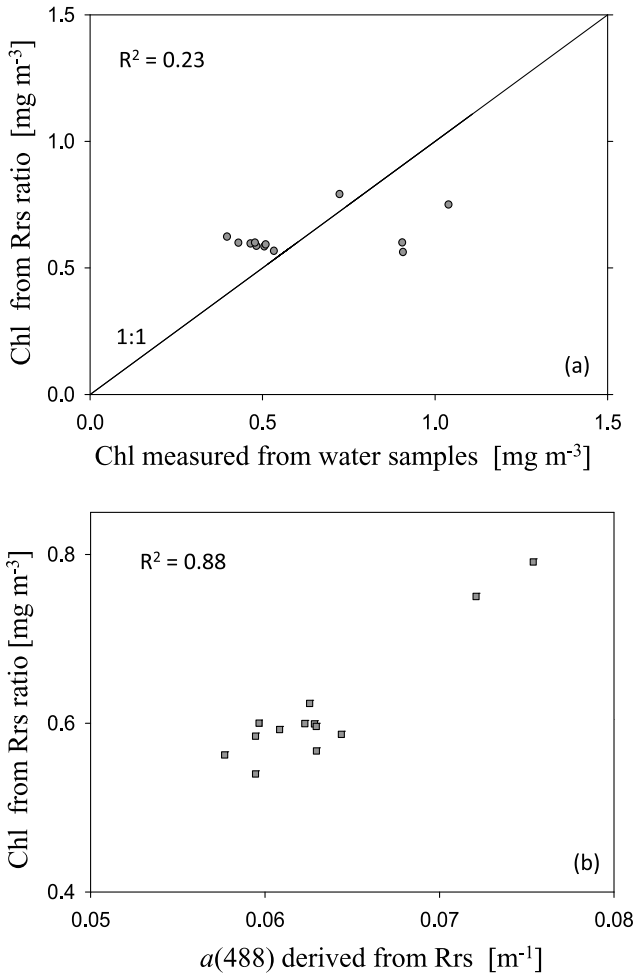

Figure 7. (a) Comparison of Chl between in situ measurements and OC3M estimates. (b) Scatterplot between QAA-derived $a(488)$ and OC3M-derived Chl.

absorption coefficient [*Lee et al.*, 1998; *Shang et al.*, 2011; *Smyth et al.*, 2002]. Consequently, if the total absorption information is not decomposed (like the simple R_{rs} ratio algorithm) into the contributions of phytoplankton and detritus-gelbstoff, optical signal of detritus-gelbstoff will be inferred as Chl, and errors will be propagated to PP that uses such Chl values as an input. As a simple test, we replaced the empirically derived Chl in equation (6) with the QAA-derived Aph, and an R^2 value of 0.69 was obtained. Separately, when in situ Chl value was used as input in the Chl-PP models, the R^2 value also improved significantly (R^2 = 0.82 (0.71), N = 12, between measured PP_{eu} and Chl-PP_B (Chl-PP_A)). These results clearly indicate the importance and significance in removing detritus-gelbstoff in ocean color remote sensing for biogeochemical studies even for oceanic waters [*Carder et al.*, 1989; *Siegel et al.*, 2005].

[36] Although better R^2 values were found for Chl-PP estimates when measured Chl were used as inputs, estimation of primary production based on Chl faces more challenges when available information is remotely measured ocean color radiance. This is because that quantitative PP estimation using a Chl-PP model depends on the accuracy of both Chl and the physiological parameters (e.g., P^B_{opt}, G_{max}), if we assume the light information could be well determined. The P^B_{opt} value, however, is far from a constant and depends on many factors [*Balch et al.*, 1992; *Behrenfeld and Falkowski*, 1997b; *Cleveland et al.*, 1989; *Sosik*, 1996; *Uitz et al.*, 2008]. One of those is the chlorophyll-specific absorption coefficient, which varies both temporally and spatially, or with phytoplankton sizes or functional types [*Bricaud et al.*, 1995; *Ciotti et al.*, 2002; *Sathyendranath et al.*, 1987]. This variation, at present, could not be accurately derived from remote sensing. At the same time, when Chl is derived from R_{rs}, chlorophyll-specific absorption is also associated explicitly [*Carder et al.*, 1999] or implicitly (like the OC3M algorithm for processing MODIS data). Because the model for P^B_{opt} or G_{max} and the empirical algorithm for Chl were developed independently, two separate values representing the chlorophyll-specific absorption could be embedded in the algorithms that do not necessarily match each other. Consequently a larger compound error could be introduced in the final estimated PP_{eu} from remote sensing [*Lee et al.*, 1996]. The Aph-PP approach, on the other hand, is centered on IOPs which avoids the association with the chlorophyll-specific absorption coefficient, and thus eliminates one of the large error sources when estimating the quantity of primary production from remote sensing. Therefore, from the remote sensing point of view, estimating PP with an Aph-PP approach is superior to a Chl-PP approach, as demonstrated by *Lee et al.* [1996] and *Marra et al.* [2007] as well as the larger R^2 and lower δ values in this study. Implementing an Aph-PP approach for global PP estimation, however, demands dedicated efforts to develop accurate models for phytoplankton physiological parameters (e.g., K_φ and φ_m) of global waters, as they are critical in determining primary production in a natural environment [*Behrenfeld and Falkowski*, 1997a].

4.2.2. PP in the Southern Ocean From MODIS Measurements

[37] Because the PP_{eu} values estimated from the Aph-PP scheme agreed well with sample measurements in both quantity and variability, we applied this scheme to satellite measurements to assess and explore spatial variation of PP_{eu} for the greater SO GasEx region during austral autumn 2008 despite the lack of a model for K_φ and φ_m for global waters (the φ_m value used approximates the lower limit shown by *Hiscock et al.* [2008] for the Southern Ocean). Aph-PP (equation (4)) was applied to MODIS measurements using E_0 (see section 3.2 for details) and optical properties derived from MODIS R_{rs}. Figure 8a shows the mean PP_{eu} for the period 1 March to 31 May 2008. For a visual comparison and contrast, PP_{eu} of this time window was also derived with Chl-PP_B and Chl-PP_A (Chl is derived with the OC3M algorithm) and presented in Figures 8b and 8c, respectively.

[38] Generally, with the current default values for the physiological parameters, the PP_{eu} range from Aph-PP is ~100–1000 mg C m^{-2} d^{-1}, with maximum PP_{eu} observed near the coastal region off Argentina. These values and variability are consistent with those on-deck measurements made during the cruise. However, PP_{eu} values from Aph-PP show quite a different spatial pattern (in general less spatial gradient) compared with that generated by the Chl-PP models. For instance, much higher PP_{eu} values (close to ~2000 mg C m^{-2} d^{-1}) in the coastal waters off Argentina (Figures 8b and 8c) are found from the Chl-PP scheme. On

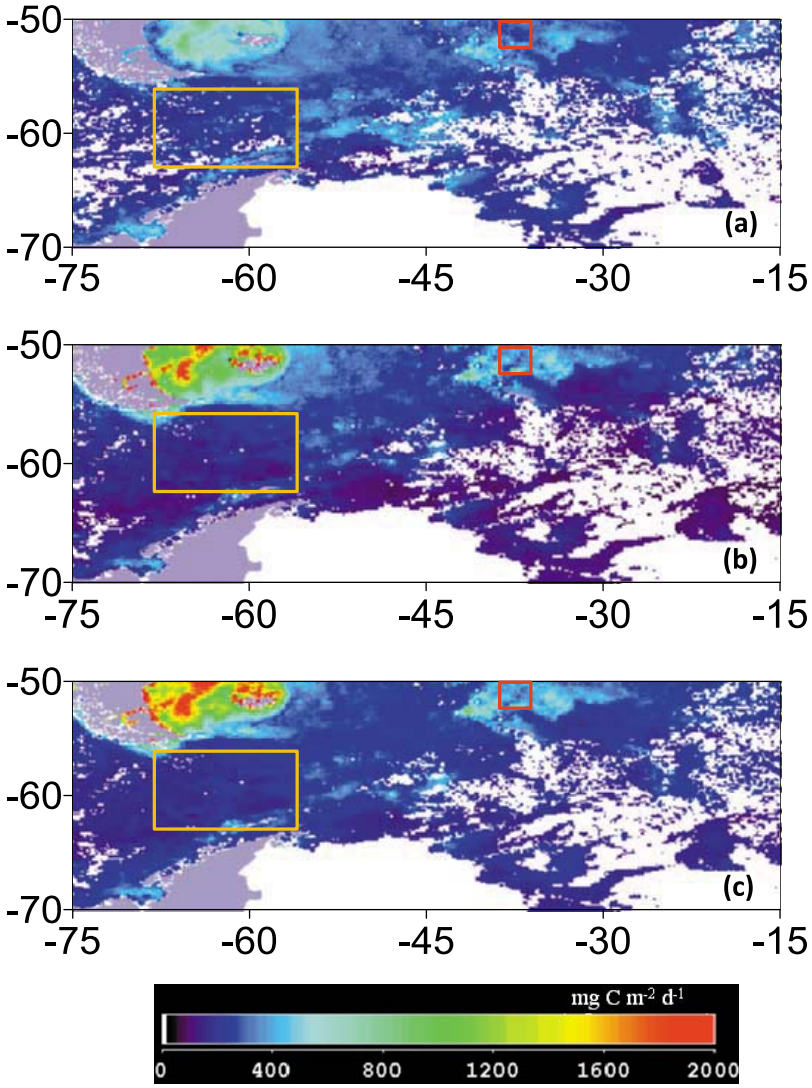

Figure 8. Spatial distribution of PP_{eu} in the Southern Ocean (austral autumn 2008): from (a) Aph-PP model, (b) Chl-PP_B model, and (c) Chl-PP_A model. The red box (illustration only) covers the SO GasEx region. Grey-colored pixels for land and white-colored pixels for ice or no data.

the other hand, PP_{eu} values from Aph-PP are much higher (~2 times) than those from Chl-PP for waters in the Drake Passage (yellow box in Figure 8). In addition, PP_{eu} from Chl-PP are generally higher than PP_{eu} from Aph-PP for waters measured during the SO GasEx (red box in Figure 8), which is consistent with the comparison shown in Figure 6. These results indicate potentially quite different PP_{eu} temporal and spatial variations in the Southern Ocean [*Arrigo et al.*, 1998, 2008] if PP_{eu} is calculated using an Aph-PP model.

[39] For the 2 days where both MODIS and in situ PP_{eu} measurements were available, PP_{eu} measured from deck incubation were ~398 mg C m^{-2} d^{-1} (day 84) and ~337 mg C m^{-2} d^{-1} (day 94). PP_{eu} from Aph-PP were ~473 mg C m^{-2} d^{-1} (day 84) and ~206 mg C m^{-2} d^{-1} (day 94), which matched the decreasing pattern over sampling locations but not the values. PP_{eu} based on Chl-PP, however, increased for the 2 days (~368 to ~476 mg C m^{-2} d^{-1} from Chl-PP_B; ~546 to ~670 mg C m^{-2} d^{-1} from Chl-PP_A). These comparisons, along with the comparisons of PP_{eu} from in situ measurement of R_{rs}, although quite limited in scale, point to a promising potential of improving the determination of primary production from remotely sensed products via the Aph-PP strategy [*Lee et al.*, 1996; *Marra et al.*, 2007].

5. Summary

[40] For measurements of both optical properties and primary production made during the Southern Ocean Gas Experiment in the austral autumn 2008, although quite limited in scale, we found that optical properties (a, a_{ph} and a_{dg}) derived from remote-sensing reflectance with the QAA scheme match well with those from in situ measurements. Discrepancies of ~10–20% (at 443 nm, $R^2 > 0.74$) between remote-sensing retrievals and ac-9 measurements (the discrepancy is larger between remote-sensing retrievals and that from water sample measurements) can be well explained by the technique used and by the natural variations of optical properties in the oceans. In sharp contrast, Chl derived empirically from R_{rs} with the OC3M algorithm did not

capture the variation of chlorophyll concentration measured from water samples (R^2 = 0.23, N = 12). These results provide assurance of analytically retrieved optical properties from remote sensing reflectance for waters in the Southern Ocean. The low correlation between remote-sensing Chl and in situ HPLC Chl casts high uncertainties in estimated primary production (PP_{eu}) when this empirically derived Chl is used as an input in Chl-PP models to estimate PP_{eu} ($R^2 < 0.5$ for the two Chl-PP models used, N = 13). But, when the primary production (PP_{eu}) was estimated using analytically derived phytoplankton absorption coefficient, the R^2 value became 0.74 (N = 13) between estimated and measured PP_{eu}. In addition, lower percentage difference (δ) was found between PP_{eu} estimated by Aph-PP and PP_{eu} measured in situ. These results suggest significant consequences in the estimation of the contribution of the biological pump to global carbon cycles if primary production of the global oceans is estimated with an Aph-PP approach.

[41] The results presented here further highlight the importance of correcting the optical impacts of detritus-gelbstoff in ocean color remote sensing even for oceanic waters and demonstrate promising potentials of using analytically derived phytoplankton absorption coefficient as an input to improve the estimation of basin-scale primary production from remote sensing. To reach this ultimate goal, in addition to obtain accurate retrieval of optical properties from ocean color measurements, it demands dedicated efforts to reliably estimate the physiological parameters (e.g., quantum yield of photosynthesis) from remote sensing also.

Appendix A: Time-, Wavelength-, and Depth-Integrated *Arrigo et al.* [2008] PP Model

[42] Based on equation (7) of *Arrigo et al.* [2008], assuming vertically homogeneous water and that both chlorophyll concentration and water temperature do not change in a day, daily water column primary production can be expressed as

$$\mathrm{PP_{eu}} = \mathrm{Chl}\,\frac{C}{\mathrm{Chl}}\,G_{\max}\int_{z=0}^{z_m} L(z)\,dz. \tag{A1}$$

Here z_m is taken as 50 m for the study. C/Chl is the phytoplankton carbon to Chl ratio and is 88.5 (g:g).

[43] $G_{\max}$ is the daily maximum growth rate, and is expressed as

$$G_{\max} = G_0\,\exp(-r\,SST), \tag{A2}$$

with G_0 = 0.59 $\mathrm{day^{-1}}$, and r = 0.0633°$\mathrm{C^{-1}}$. $G_{\max}$ approximates 0.81 $\mathrm{day^{-1}}$ for the in situ measurements (calculated for SST = 5°C).

[44] $L(z)$ is the "light limitation term," and its vertical distribution is

$$L(z) = 1 - \exp\left(-\frac{\mathrm{PUR}(z)}{E'_k(z)}\right), \tag{A3}$$

with PUR the "photosynthetically usable radiation" and E'_k the "photoacclimation parameter."

[45] PUR is calculated as

$$\mathrm{PUR}(z) = \int_{400}^{700} E_d(\lambda, z)\,a^+_{ph}(\lambda)\,d\lambda, \tag{A4}$$

with $E_d(\lambda, z)$ the spectral downwelling irradiance at depth z, and $a^+_{ph}(\lambda)$ the 440 nm normalized $a_{ph}(\lambda)$. Since Chl derived from R_{rs} is generally around 0.5 mg $\mathrm{m^{-3}}$ in this study, $a^+_{ph}(\lambda)$ is modeled with Chl = 0.5 mg $\mathrm{m^{-3}}$ using the formula of *Bricaud et al.* [1998].

[46] E'_k is calculated from

$$E'_k(z) = \frac{E'_{k\max}}{1 + 2\exp(-B\ \mathrm{PUR}(z))}, \tag{A5}$$

with $E'_{k\ \max}$ = 80 μEin $\mathrm{m^{-2}\ s^{-1}}$, and B is 0.052 corresponding to this $E'_{k\max}$.

[47] The vertical distribution of $E_d(\lambda, z)$ is calculated from

$$E_d(\lambda, z) = E_d(\lambda, 0)\exp\left(-\frac{\overline{K}_d(\lambda)}{\cos(\overline{\theta}_w)}\,z\right), \tag{A6}$$

with $\overline{\theta}_w$ the daily average solar zenith angle just below the surface (taken as 45° for this study). $\overline{K}_d(\lambda)$ is the average diffuse attenuation coefficient corresponding to Sun at noon and modeled as [*Morel and Maritorena*, 2001]

$$\overline{K}_d(\lambda) = K_w(\lambda) + \chi(\lambda)\,(Chl)^{e(\lambda)}. \tag{A7}$$

$E_d(\lambda, z)$ at surface ($E_d(\lambda, 0)$) is calculated by scaling measured E_0

$$E_d(\lambda, 0) = E_0\,E^+_d(\lambda), \tag{A8}$$

with $E^+_d(\lambda)$ the normalized spectral shape of $E_d(\lambda, 0)$ and calculated with Radtran [*Gregg and Carder*, 1990]. The units of PUR used in equation (A5) is μEin $\mathrm{m^{-2}\ s^{-1}}$ in order to match the units of $E'_{k\max}$.

[48] To facilitate calculation using data products from MODIS, the integration term on the right side of equation (A1), which is associated with equations (A3)–(A8), is reduced to

$$\int_{z=0}^{50} L(z)dz \approx \frac{5.86\,E_0}{-0.71 + 0.29\,E_0 + 5.04\,\mathrm{Chl}}. \tag{A9}$$

The error is about ±10% between the integration obtained from equation (A9) and that obtained through equations (A3)–(A8). Note that the coefficients in equation (A9) are corresponding to $\overline{\theta}_w = 45°$, and the range of Chl is 0.3–2.0 mg $\mathrm{m^{-3}}$ and the range of E_0 is 5 to 30 Ein $\mathrm{m^{-2}\ d^{-1}}$, values cover that reported in this study.

[49] **Acknowledgments.** We thank the captain and the crew of R/V *Ronald H. Brown* for excellent support during the SO GasEx, and we are thankful for the support from NASA's Ocean Biology and Biogeochemistry Program (Del Castillo, Hargreaves, Lance, Lee, Miller, Twardowski, and Vaillancourt) and that from NSF-China (40976068, 40821063; Shang). We also thank NASA's Ocean Biology Processing Group for providing satellite data products. Comments and suggestions from two anonymous reviewers are greatly appreciated.

References

Antoine, D., A. Morel, and J.-M. Andre (1995), Algal pigment distribution and primary production in the eastern Mediterranean as derived from coastal zone color scanner observations, *J. Geophys. Res.*, *100*(C8), 16,193–16,209, doi:10.1029/95JC00466.

Antoine, D., J.-M. Andre, and A. Morel (1996), Oceanic primary production: 2. Estimation at global scale from satellite (coastal zone color scanner) chlorophyll, *Global Biogeochem. Cycles*, *10*(1), 57–69, doi:10.1029/95GB02832.

Arrigo, K., D. Worthen, A. Schnell, and M. P. Lizotte (1998), Primary production in Southern Ocean waters, *J. Geophys. Res.*, *103*(C8), 15,587–15,600, doi:10.1029/98JC00930.

Arrigo, K. R., G. L. v. Dijken, and S. Bushinsky (2008), Primary production in the Southern Ocean, 1997–2006, *J. Geophys. Res.*, *113*, C08004, doi:10.1029/2007JC004551.

Austin, R. W. (1974), Inherent spectral radiance signatures of the ocean surface, in *Ocean Color Analysis*, edited by S. W. Duntley, pp. 1–20, Scripps Inst. of Oceanogr, San Diego, Calif.

Balch, W. M., and C. F. Byrne (1994), Factors affecting the estimate of primary production from space, *J. Geophys. Res.*, *99*(C4), 7555–7570, doi:10.1029/93JC03091.

Balch, W. M., R. W. Epply, and M. R. Abbott (1989), Remote sensing of primary production—Part II. A semi-analytical algorithm based on pigments, temperature and light, *Deep Sea Res. Part A*, *36*(8), 1201–1217, doi:10.1016/0198-0149(89)90101-5.

Balch, W. M., R. Evans, J. Brown, G. Feldman, C. McClain, and W. Esaias (1992), The remote sensing of ocean primary productivity: Use of a new data compilation to test satellite algorithms, *J. Geophys. Res.*, *97*(C2), 2279–2293, doi:10.1029/91JC02843.

Behrenfeld, M. J., and P. G. Falkowski (1997a), A consumer's guide to phytoplankton primary productivity models, *Limnol. Oceanogr.*, *42*(7), 1479–1491, doi:10.4319/lo.1997.42.7.1479.

Behrenfeld, M. J., and P. G. Falkowski (1997b), Photosynthetic rates derived from satellite-based chlorophyll concentration, *Limnol. Oceanogr.*, *42*(1), 1–20, doi:10.4319/lo.1997.42.1.0001.

Behrenfeld, M. J., et al. (1998), Toward a consensus productivity algorithm for SeaWiFS, in *Satellite Primary Productivity Data and Algorithm Development: A Science Plan for Mission to Planet Earth*, edited by S. B. Hooker and E. R. Firestone, *SeaWiFS Tech. Rep. 42*, pp. 2–17, NASA Goddard Space Flight Cent., Greenbelt, Md.

Behrenfeld, M. J., W. E. Esaias, and K. R. Turpie (2002), Assessment of primary production at the global scale, in *Phytoplankton Productivity: Carbon Assimilation in Marine and Freshwater Ecosystems*, edited by P. J. l. Williams, D. N. Thomas, and C. S. Reynolds, pp. 156–186, Blackwell Sci., Malden, Mass.

Behrenfeld, M. J., R. T. O'Malley, D. A. Siegel, C. R. McClain, J. L. Sarmiento, G. C. Feldman, A. J. Willigan, P. G. Falkowski, R. M. Letelier, and E. S. Boss (2006), Climate-driven trends in contemporary ocean productivity, *Nature*, *444*, 752–755, doi:10.1038/nature05317.

Bricaud, A., M. Babin, A. Morel, and H. Claustre (1995), Variability in the chlorophyll-specific absorption coefficients of natural phytoplankton: Analysis and parameterization, *J. Geophys. Res.*, *100*(C7), 13,321–13,332, doi:10.1029/95JC00463.

Bricaud, A., A. Morel, M. Babin, K. Allali, and H. Claustre (1998), Variations of light absorption by suspended particles with chlorophyll a concentration in oceanic (case 1) waters: Analysis and implications for bio-optical models, *J. Geophys. Res.*, *103*(C13), 31,033–31,044, doi:10.1029/98JC02712.

Bricaud, A., M. Babin, H. Claustre, J. Ras, and F. Tieche (2010), Light absorption properties and absorption budget of Southeast Pacific waters, *J. Geophys. Res.*, *115*, C08009, doi:10.1029/2009JC005517.

Campbell, J., et al. (2002), Comparison of algorithms for estimating ocean primary production from surface chlorophyll, temperature, and irradiance, *Global Biogeochem. Cycles*, *16*(3), 1035, doi:10.1029/2001GB001444.

Carder, K. L., and R. G. Steward (1985), A remote-sensing reflectance model of a red tide dinoflagellate off west Florida, *Limnol. Oceanogr.*, *30*(2), 286–298, doi:10.4319/lo.1985.30.2.0286.

Carder, K. L., R. G. Steward, G. R. Harvey, and P. B. Ortner (1989), Marine humic and fulvic acids: Their effects on remote sensing of ocean chlorophyll, *Limnol. Oceanogr.*, *34*(1), 68–81, doi:10.4319/lo.1989.34.1.0068.

Carder, K. L., F. R. Chen, Z. P. Lee, S. K. Hawes, and D. Kamykowski (1999), Semianalytic Moderate-Resolution Imaging Spectrometer algorithms for chlorophyll-a and absorption with bio-optical domains based on nitrate-depletion temperatures, *J. Geophys. Res.*, *104*(C3), 5403–5421, doi:10.1029/1998JC900082.

Carr, M., et al. (2006), A comparison of global estimates of marine primary production from ocean color, *Deep Sea Res. Part II*, *53*(5–7), 741–770, doi:10.1016/j.dsr2.2006.01.028.

Ciotti, A. M., M. R. Lewis, and J. J. Cullen (2002), Assessment of the relationships between domininant cell size in natural phytoplankton communities and spectral shape of the absorption coefficient, *Limnol. Oceanogr.*, *47*(2), 404–417, doi:10.4319/lo.2002.47.2.0404.

Clementson, L. A., J. S. Parslow, A. R. Turnbull, D. C. McKenzie, and C. E. Rathbone (2001), Optical properties of waters in the Australasian sector of the Southern Ocean, *J. Geophys. Res.*, *106*(C12), 31,611–31,625, doi:10.1029/2000JC000359.

Cleveland, J. S., M. J. Perry, D. A. Kiefer, and M. C. Talbot (1989), Maximal quantum yield of photosynthesis in the northwestern Sargasso Sea, *J. Mar. Res.*, *47*(4), 869–886, doi:10.1357/002224089785076055.

Cullen, J. J. (1990), On models of growth and photosynthesis in phytoplankton, *Deep Sea Res. Part A*, *37*(4), 667–683, doi:10.1016/0198-0149(90)90097-F.

Dierssen, H. M., and R. C. Smith (2000), Bio-optical properties and remote sensing ocean color algorithms for Antarctic Peninsula waters, *J. Geophys. Res.*, *105*(C11), 26,301–26,312, doi:10.1029/1999JC000296.

Ducklow, H. W. (2003), Biogeochemical provinces: Towards a JGOFS synthesis, in *Ocean Biogeochemistry: A Synthesis of the Joint Global Ocean Flux Study (JGOFS)*, edited by M. J. Fashman, pp. 3–17, Springer, Berlin.

Falkowski, P. G. (1998), Using satellite data to derive primary productivity in the world ocean, in *Satellite Primary Productivity Data and Algorithm Development: A Science Plan for Mission to Planet Earth*, edited by S. B. Hooker and E. R. Firestone, *SeaWiFS Tech. Rep. 42*, pp. 18–25, NASA Goddard Space Flight Cent., Greenbelt, Md.

Falkowski, P. G., E. A. Laws, R. T. Barber, and J. W. Murray (2003), Phytoplankton and their role in primary, new, and export production, in *Ocean Biogeochemistry: A Synthesis of the Joint Global Ocean Flux Study (JGOFS)*, edited by M. J. Fashman, pp. 99–121, Springer, Berlin.

Friedrichs, M. A. M., et al. (2009), Assessing the uncertainties of model estimates of primary productivity in the tropical Pacific Ocean, *J. Mar. Syst.*, *76*(1–2), 113–133, doi:10.1016/j.jmarsys.2008.05.010.

Garcia, C. A. E., V. M. T. Garcia, and C. R. McClain (2005), Evaluation of SeaWiFS chlorophyll algorithms in the Southwestern Atlantic and Southern Oceans, *Remote Sens. Environ.*, *95*(1), 125–137, doi:10.1016/j.rse.2004.12.006.

Gregg, W. W., and K. L. Carder (1990), A simple spectral solar irradiance model for cloudless maritime atmospheres, *Limnol. Oceanogr.*, *35*(8), 1657–1675, doi:10.4319/lo.1990.35.8.1657.

Halsey, K. H., A. J. Milligan, and M. J. Behrenfeld (2010), Physiological optimization underlies growth rate-independent chlorophyll-specific gross and net primary production, *Photosynth. Res.*, *103*, 125–137, doi:10.1007/s11120-009-9526-z.

Hargreaves, B., and A. Vaidya (2010), Rigorous calibration of an improved filter pad method for phytoplankton spectral absorption and application to SOGASEX, paper presented at Ocean Optics 2010, Oceanogr. Soc., Anchorage, Alaska.

Hiscock, M. R., V. P. Lance, A. M. Apprill, R. R. Bidigare, Z. I. Johnson, B. G. Mitchell, J. Walker, O. Smith, and R. T. Barber (2008), Photosynthetic maximum quantum yield increases are an essential component of the Southern Ocean phytoplankton response to iron, *Proc. Natl. Acad. Sci. U. S. A.*, *105*(12), 4775–4780, doi:10.1073/pnas.0705006105.

Hu, C., Z. Lee, F. E. Muller-Karger, K. L. Carder, and J. J. Walsh (2006), Ocean color reveals phase shift between marine plants and yellow substance, *IEEE Geosci. Remote Sens. Lett.*, *3*(2), 262–266, doi:10.1109/LGRS.2005.862527.

International Ocean-Colour Coordinating Group (IOCCG) (2006), Remote sensing of inherent optical properties: Fundamentals, tests of algorithms, and applications, edited by Z.-P. Lee, *IOCCG Rep. 5*, Dartmouth, N. S., Canada.

Ishizaka, J. (1998), Spatial distribution of primary production off Sanriku, northwestern Pacific, during spring estimated by Ocean Color and Temperature Scanner (OCTS), *J. Oceanogr.*, *54*(5), 553–564, doi:10.1007/BF02742457.

Lee, Z. P., K. L. Carder, J. Marra, R. G. Steward, and M. J. Perry (1996), Estimating primary production at depth from remote sensing, *Appl. Opt.*, *35*(3), 463–474, doi:10.1364/AO.35.000463.

Lee, Z. P., K. L. Carder, R. G. Steward, T. G. Peacock, C. O. Davis, and J. S. Patch (1998), An empirical algorithm for light absorption by ocean water based on color, *J. Geophys. Res.*, *103*(C12), 27,967–27,978, doi:10.1029/98JC01946.

Lee, Z. P., K. L. Carder, and R. Arnone (2002), Deriving inherent optical properties from water color: A multi-band quasi-analytical algorithm for optically deep waters, *Appl. Opt.*, *41*(27), 5755–5772, doi:10.1364/AO.41.005755.

Lee, Z. P., K. Du, R. Arnone, S. C. Liew, and B. Penta (2005), Penetration of solar radiation in the upper ocean: A numerical model for oceanic and

coastal waters, *J. Geophys. Res.*, *110*, C09019, doi:10.1029/2004JC002780.
Lee, Z. P., A. Weidemann, J. Kindle, R. Arnone, K. L. Carder, and C. Davis (2007), Euphotic zone depth: Its derivation and implication to ocean-color remote sensing, *J. Geophys. Res.*, *112*, C03009, doi:10.1029/2006JC003802.
Lee, Z. P., Y.-H. Ahn, C. Mobley, and R. Arnone (2010a), Removal of surface-reflected light for the measurement of remote-sensing reflectance from an above-surface platform, *Opt. Express*, *18*(25), 26,313–26,342, doi:10.1364/OE.18.026313.
Lee, Z. P., R. Arnone, C. Hu, P. J. Werdell, and B. Lubac (2010b), Uncertainties of optical parameters and their propagations in an analytical ocean color inversion algorithm, *Appl. Opt.*, *49*(3), 369–381, doi:10.1364/AO.49.000369.
Lee, Z. P., K. Du, K. J. Voss,G. Zibordi, B. Lubac, R. Arnone, and A. Weidemann (2011), An IOP-centered approach to correct the angular effects in water-leaving radiance, *Appl. Opt.*, in press.
Leymarie, E., D. Doxaran, and M. Babin (2010), Uncertainties associated to measurements of inherent optical properties in natural waters, *Appl. Opt.*, *49*(28), 5415–5436, doi:10.1364/AO.49.005415.
Longhurst, A. R., S. Sathyendranath, T. Platt, and C. Caverhill (1995), An estimate of global primary production in the ocean from satellite radiometer data, *J. Plankton Res.*, *17*(6), 1245–1271, doi:10.1093/plankt/17.6.1245.
Marra, J., C. Ho, and C. Trees (2003), An alternative algorithm for the calculation of primary productivity from remote sensing data, *Tech. Rep. LDEO-2003-1*, 27 pp., Lamont-Doherty Earth Obs., Palisades, N. Y.
Marra, J., C. C. Trees, and J. E. O'Reilly (2007), Phytoplankton pigment absorption: A strong predictor of primary productivity in the surface ocean, *Deep Sea Res. Part I*, *54*(2), 155–163, doi:10.1016/j.dsr.2006.12.001.
Marrari, M., C. Hu, and K. Daly (2006), Validation of SeaWiFS chlorophyll a concentrations in the Southern Ocean: A revisit, *Remote Sens. Environ.*, *105*(4), 367–375, doi:10.1016/j.rse.2006.07.008.
McClain, C. R., J. R. Christian, S. Signorini, M. R. Lewis, I. Asnauma, D. Turk, and C. Dupouy-Douchement (2002), Satellite ocean-color observations of the tropical Pacific Ocean, *Deep Sea Res. Part II*, *49*(13–14), 2533–2560, doi:10.1016/S0967-0645(02)00047-4.
Miller, R. L., M. Belz, C. D. Castillo, and R. Trzask (2002), Determining CDOM absorption spectra in diverse coastal environments using a multiple pathlength, liquid core waveguide system, *Cont. Shelf Res.*, *22*(9), 1301–1310, doi:10.1016/S0278-4343(02)00009-2.
Mitchell, B. G., and O. Holm-Hansen (1990), Bio-optical properties of Antarctic Peninsula waters: Differentiation from temperate ocean models, *Deep Sea Res. Part A*, *38*(8–9), 1009–1028, doi:10.1016/0198-0149(91)90094-V.
Mitchell, B. G., E. A. Brody, O. Holm-Hansen, C. McClain, and J. Bishop (1991), Light limitation of phytoplankton biomass and macronutrient utilization in the Southern Ocean, *Limnol. Oceanogr.*, *36*(8), 1662–1677, doi:10.4319/lo.1991.36.8.1662.
Moore, J. K., and M. R. Abbott (2000), Phytoplankton chlorophyll distributions and primary production in the Southern Ocean, *J. Geophys. Res.*, *105*(C12), 28,709–28,722, doi:10.1029/1999JC000043.
Morel, A. (1974), Optical properties of pure water and pure sea water, in *Optical Aspects of Oceanography*, edited by N. G. Jerlov and E. S. Nielsen, pp. 1–24, Academic, New York.
Morel, A., and J. F. Berthon (1989), Surface pigments, algal biomass profiles, and potential production of the euphotic layer: Relationships reinvestigated in view of remote-sensing applications, *Limnol. Oceanogr.*, *34*(8), 1545–1562, doi:10.4319/lo.1989.34.8.1545.
Morel, A., and B. Gentili (2009), A simple band ratio technique to quantify the colored dissolved and detrital organic material from ocean color remotely sensed data, *Remote Sens. Environ.*, *113*(5), 998–1011, doi:10.1016/j.rse.2009.01.008.
Morel, A., and S. Maritorena (2001), Bio-optical properties of oceanic waters: A reappraisal, *J. Geophys. Res.*, *106*(C4), 7163–7180, doi:10.1029/2000JC000319.
Morel, A., B. Gentili, H. Claustre, A. Babin, A. Bricaud, J. Ras, and F. Tieche (2007), Optical properties of the "clearest" natural waters, *Limnol. Oceanogr.*, *52*(1), 217–229, doi:10.4319/lo.2007.52.1.0217.
Ondrusek, M. E., R. R. Bidigare, K. Waters, and D. M. Kar (2001), A predictive model for estimating rates of primary production in the subtropical North Pacific Ocean, *Deep Sea Res. Part II*, *48*(8–9), 1837–1863, doi:10.1016/S0967-0645(00)00163-6.
O'Reilly, J. E., et al. (2000), *SeaWiFS Postlaunch Calibration and Validation Analyses, Part 3*, edited by S. B. Hooker and E. R. Firestone, *SeaWiFS Postlaunch Tech. Rep. 11*, 58 pp., NASA Goddard Space Flight Cent., Greenbelt, Md.
Platt, T., and S. Sathyendranath (1988), Oceanic primary production: Estimation by remote sensing at local and regional scales, *Science*, *241*(4873), 1613–1620, doi:10.1126/science.241.4873.1613.
Pope, R., and E. Fry (1997), Absorption spectrum (380–700 nm) of pure waters: Part II. Integrating cavity measurements, *Appl. Opt.*, *36*(33), 8710–8723, doi:10.1364/AO.36.008710.
Sabine, C. L., et al. (2004), The Oceanic sink for anthropogenic CO_2, *Science*, *305*(5682), 367–371, doi:10.1126/science.1097403.
Sathyendranath, S., L. Lazzara, and L. Prieur (1987), Variations in the spectral values of specific absorption of phytoplankton, *Limnol. Oceanogr.*, *32*(2), 403–415, doi:10.4319/lo.1987.32.2.0403.
Sathyendranath, S., T. Platt, E. P. W. Horne, W. G. Harrison, O. Ulloa, R. Outerbridge, and N. Hoepffner (1991), Estimation of new production in the ocean by compound remote sensing, *Nature*, *353*, 129–133, doi:10.1038/353129a0.
Sathyendranath, S., A. R. Longhurst, C. Caverhill, and T. Platt (1995), Regionally and seasonally differentiated primary production in the North Atlantic, *Deep Sea Res. Part I*, *42*(10), 1773–1802, doi:10.1016/0967-0637(95)00059-F.
Schlitzer, R. (2002), Carbon export fluxes in the Southern Ocean: Results from inverse modeling and comparison with satellite-based estimates, *Deep Sea Res. Part II*, *49*(9–10), 1623–1644, doi:10.1016/S0967-0645(02)00004-8.
Shang, S. L., Q. Dong, Z. P. Lee, Y. Li, Y. S. Xie, and M. J. Behrenfeld (2011), MODIS observed phytoplankton dynamics in the Taiwan Strait: An absorption-based analysis, *Biogeosciences*, *8*, 841–850, doi:10.5194/bg-8-841-2011.
Siegel, D. A., S. Maritorena, N. B. Nelson, and M. J. Behrenfeld (2005), Independence and interdependencies among global ocean color properties: Reassessing the bio-optical assumption, *J. Geophys. Res.*, *110*, C07011, doi:10.1029/2004JC002527.
Smyth, T. J., S. B. Groom, D. G. Cummings, and C. A. Llewellyn (2002), Comparison of SeaWiFS bio-optical chlorophyll-a algorithms within the OMEXII programme, *Int. J. Remote Sens.*, *23*(11), 2321–2326, doi:10.1080/01431160110109624.
Sosik, H. M. (1996), Bio-optical modeling of primary production: Consequences of variability in quantum yield and specific absorption, *Mar. Ecol. Prog. Ser.*, *143*, 225–238, doi:10.3354/meps143225.
Stuart, V., S. Sathyendranath, T. Platt, H. Maass, and B. Irwin (1998), Pigments and species composition of natural phytoplankton populations: Effect on the absorption spectra, *J. Plankton Res.*, *20*(2), 187–217, doi:10.1093/plankt/20.2.187.
Sullivan, C. W., K. R. Arrigo, C. R. McClain, J. C. Comiso, and J. Firestone (1993), Distributions of phytoplankton blooms in the Southern Ocean, *Science*, *262*(5141), 1832–1837, doi:10.1126/science.262.5141.1832.
Sullivan, J. M., M. S. Twardowski, J. R. V. Zaneveld, C. M. Moore, A. H. Barnard, P. L. Donaghay, and B. Rhoades (2006), Hyperspectral temperature and salt dependencies of absorption by water and heavy water in the 400–750 nm spectral range, *Appl. Opt.*, *45*(21), 5294–5309, doi:10.1364/AO.45.005294.
Takahashi, M., S. C. Sutherland, and C. Sweeney (2002), Global sea-air CO_2 flux based on climatological surface ocean pCO_2, and seasonal biological and temperature effects, *Deep Sea Res. Part II*, *49*(9–10), 1601–1622, doi:10.1016/S0967-0645(02)00003-6.
Takahashi, T., R. H. Wanninkhof, R. A. Feely, R. F. Weiss, D. W. Chipman, N. Bates, J. Olafsson, C. Sabine, and S. C. Sutherland (1999), Net sea-air CO_2 flux over the global oceans: An improved estimate based on the sea-air pCO_2 difference, paper presented at Second International Symposium: CO_2 in the Oceans, Cent. for Global Environ. Res., Tsukuba, Japan.
Tassan, S., and G. M. Ferrari (1995), An alternative approach to absorption measurements of aquatic particles retained on filters, *Limnol. Oceanogr.*, *40*(8), 1358–1368, doi:10.4319/lo.1995.40.8.1358.
Tassan, S., B. G. Mitchell, D. Stramski, and A. Bricaud (1997), Light absorption measurements of aquatic particles: Status and prospects, paper presented at IGARSS '97, Inst. of Electr. and Electron. Eng., Singapore.
Treguer, P., and P. Pondaven (2002), Climate changes and the carbon cycle in the Southern Ocean: A step forward, *Deep Sea Res. Part II*, *49*(9–10), 1597–1600, doi:10.1016/S0967-0645(02)00002-4.
Uitz, J., Y. Huot, F. Bruyant, M. Babin, and H. Claustre (2008), Relating phytoplankton photophysiological properties to community structure on large scales, *Limnol. Oceanogr.*, *53*(2), 614–630, doi:10.4319/lo.2008.53.2.0614.
Vaidya, A. (2010), Improved filterpad measurements for spectral absorption by phytoplankton, M.S. thesis, 81 pp., Lehigh Univ., Bethlehem, Pa.
Zaneveld, J. R. V., J. C. Kitchen, and C. C. Moore (1994), Scattering error correction of reflecting-tube absorption meters, paper presented at Ocean Optics XII, Soc. of Photo-Opt. Instrum. Eng., Bergen, Norway.

C. Del Castillo, Ocean Remote Sensing Group, Applied Physics Laboratory, Johns Hopkins University, 11100 Johns Hopkins Rd., Laurel, MD 20723, USA.

S. Freeman and M. Twardowski, Department of Research, WET Labs, Inc., 70 Dean Knauss Dr., Narragansett, RI 02882, USA.

B. R. Hargreaves, Department of Earth and Environmental Sciences, Lehigh University, 1 West Packer Ave., Bethlehem, PA 18015, USA.

V. P. Lance, Science Systems and Applications, Inc., NASA Goddard Space Flight Center, Mail Code 130, Greenbelt, MD 20771, USA.

Z. Lee, Geosystems Research Institute, Mississippi State University, Bldg. 1103, Rm. 233, Stennis Space Center, MS 39529, USA. (zplee@ngi.msstate.edu)

B. Lubac, Environnements et Paléoenvironnements Océaniques et Continentaux, UMR 5805, University of Bordeaux1, Avenue des Facultés, F-33405 Talence CEDEX, France.

R. Miller, Institute for Coastal Science and Policy, East Carolina University, 379 Flanagan Bldg., Suite 250, Greenville, NC 27858, USA.

S. Shang and G. Wei, State Key Laboratory of Marine Environmental Science, Xiamen University, Zeng Cheng Kui Building, 422 Siming South Rd., Xiamen 361005, China.

R. Vaillancourt, Department of Earth Sciences, Millersville University of Pennsylvania, P.O. Box 1002, Millersville, PA 17551, USA.